RSC Applied Interfaces

ROYAL SOCIETY OF CHEMISTRY

PAPER

View Article Online
View Journal | View Issue

Cite this: *RSC Appl. Interfaces*, 2025, **2**, 373

Exploring substituent effects in reversible photoswitchable low molecular weight arylazoisoxazole adhesives†

Luca Burg, [ab] Luuk Kortekaas, [c] Anna Gibalova, [d] Constantin Daniliuc, [b] Janis Heßling, [e] Monika Schönhoff [ae] and Bart Jan Ravoo *[ab]

Received 8th November 2024,
Accepted 9th December 2024

DOI: 10.1039/d4lf00376d

rsc.li/RSCApplInter

The design of reusable responsive materials is of utmost importance to reduce the unsustainable use of valuable resources. Inspired by our initial work on the application of arylazoisoxazoles (AIZ) as reusable photoresponsive adhesives, we aim to uncover generalizations to their adhesive properties and optimize their molecular design. To achieve this goal, a molecular library of AIZ with different substitution patterns has been synthesized and examined for their adhesive properties. Several of the photoreversible low molecular weight adhesives in the library exhibited significantly enhanced (> 500%) weight-bearing capacities. This study broadens the understanding of AIZ as photoresponsive adhesives, shedding light on their limitations and the opportunities to improve their performance alike.

Introduction

Over the past decades, the development of functional adhesives has gained an increasing interest as they play a vital role in the current technological landscape. With technological progress, the increasing demands are often not just met through enhancing properties, but also in introducing new characteristics, *e.g.*, reusability and addressability for a wider range of potential "on-demand" applications. To achieve this, research has been focusing on approaches to create materials that respond to external stimuli such as pH,[1] light,[2] voltage[3,4] or temperature.[5]

In some cases, nature is particularly inspiring to design reusable materials, as evidenced in attempting to mimic the pH-dependent adhesive strength of mussels,[6] or the reversible adhesion used by geckos,[7] and with various other reversible adhesive systems having been described to date.[8] Stimuli such as the pH, heat or electrical current are all limited to specific conditions and applications, shifting the attention towards light as a versatile stimulus, which is flexibly applicable in comparison. Besides its ubiquitous availability, light is a particularly non-invasive stimulus that is both easily and safely applicable as well as non-destructive and compatible with a wide range of materials. In contrast to thermal approaches, light-responsive control is of particular interest as the associated biological, physical and chemical properties can be modulated under spatiotemporal control and at distinct wavelengths.[9] The control over this stimulus is thus substantially higher and opens a window for application in many materials that are thermally inaccessible due to a low heat capacity and possible thermal degradation.[10,11] Photoresponsive materials are often created by the implementation of molecular photoswitches, which typically undergo reversible structural changes initiated upon exposure to light of a suitable wavelength.[10,12,13] Since the discovery of photoisomerisation in azobenzenes[14] in 1937, the most established class of photoswitches has already been used in countless smart materials and applications.[15] Upon alternating exposure to UV and visible light, azobenzenes can be reversibly switched between the *E*- and *Z*-isomers. Due to the distinct difference in the isomeric geometries, this change often results in a dramatic change of material properties, which enables surfaces with reversibly switchable wettability,[16] polymers with light-responsive adhesive properties,[17,18] the manipulation of biological properties such as membrane morphology[19] or phase change materials to store and release energy.[20] Despite the general success of azobenzene application, room for improvement is still available, such as photocontrol by visible light towards biological applications[21] or the enhancement of

[a] *Center for Soft Nanoscience, University of Münster, Busso-Peus-Straße 10, 48149 Münster, Germany. E-mail: b.j.ravoo@uni-muenster.de*
[b] *Organic Chemistry Institute, University of Münster, Corrensstraße 36, 48149 Münster, Germany*
[c] *Faculty of Science and Engineering, Materials Chemistry, University of Groningen, Nijenborgh 3, 9747 Groningen, Netherlands*
[d] *Fraunhofer Institute for Manufacturing Technology and Advanced Materials, Wiener Straße 12, 28359 Bremen, Germany*
[e] *Institute of Physical Chemistry, University of Münster, Corrensstraße 28/30, 48149 Münster, Germany*

† Electronic supplementary information (ESI) available: 2379009–2379014. For the ESI and crystallographic data in CIF or other electronic format see DOI: https://doi.org/10.1039/d4lf00376d

photostationary states, often achieved by using azoheteroarenes like arylazopyrazoles (AAP), to extend functional changes through near-complete photoisomerization.[2,4,12,22]

For the implementation of stimuli response to adhesives, different physical or chemical ways can be considered. Polymer systems are one of the most used adhesive material classes, using the *in situ* polymerization or the evaporation of solvents to deliver the adhesive power on demand, albeit in a non-reversible manner.[23] Thermoplastic polymers can be melted by heating, regaining their adhesive properties upon cooling.[24] Alternatively, high bonding strengths paired with photoreversible properties can be achieved in combination with certain photoswitches. For example, polymer brushes with AAP moieties combined with cyclodextrin as the host molecule were used to create a reversible host–guest driven adhesive.[8] Weis *et al.* synthesized polymers with azobenzene photoswitches, showing a solid-to-liquid phase transition triggered by light that could be applied as an adhesive.[18,25] Ito *et al.* reported a composite of methacrylate block-copolymers with AAP implemented in the side chain and showed that the fraction of photoswitches has a linear influence on the adhesive power.[26]

However, adhesive polymer systems are usually challenging to synthesize and to reversibly apply due to degradation processes.[27] Minimizing these disadvantages while maintaining enough of the adhesive strengths in low molecular weight (LMW) adhesives can be challenging but is especially promising. Despite the common decrease of adhesive strengths upon decreasing the molecular weight, the observed linearity between the fraction of switches in the polymeric material and the adhesion suggests that a more concentrated photoswitchable functionality in exclusively LMW photoswitches has the potential also for adhesives.[26] One of the most impressive LMW adhesives was reported in 2017 where crown ether derivatives were applied as a supramolecular adhesive.[28] Besides this, other remarkable examples of LMW adhesives were developed, for example, based on LMW gelators, demonstrating adhesive properties both at room temperature and under harsh conditions at −196 °C, reaching adhesive strengths of 10–60 N cm^{-2}.[29] Since then, LMW adhesives have shown their feasibility and ease of use, but a triggered switching-off of the adhesive properties is still underdeveloped. A strategy to solve this disadvantage could be the implementation of stimuli-responsive molecular switches directly in LMW adhesive structures. Akiyama *et al.* demonstrated the usability of this approach by implementing azobenzene arms in carbohydrates of different sizes. These single component LMW adhesives with reversible solid-to-liquid phase transition upon irradiation reached adhesive strengths of 10–50 N cm^{-2}.[17,30] After Venkataramani *et al.* showed the photoreversible solid-to-liquid phase transition of tripodal derivatives of another member of the azo family, the arylazoisoxazoles (AIZ),[31] our group reported photoreversible adhesives based on LMW AIZ with alkoxy sidechains.[11] The AIZ could be easily liquefied *via* UV-irradiation and solidified back repeatedly through irradiation with green light or even an acid-catalyzed pathway,[32] proving to be a highly versatile responsive adhesive.

In this work, we focused on a deeper understanding of the influence of the chemical structure of AIZ adhesives on the demonstrated adhesive properties. For this, a library of differently substituted alkoxy-AIZ and several alkoxy-AAP with varying numbers and chain lengths of substituents was

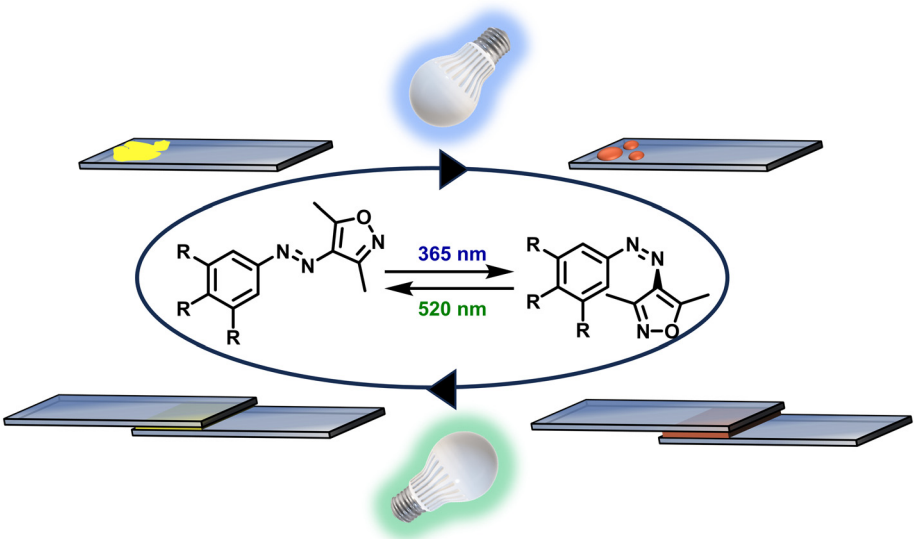

Fig. 1 Schematic overview of the use of the AIZ as a reversible adhesive. The solid *E*-AIZ can be irradiated with UV light (λ = 365 nm) to switch to the *Z*-AIZ, leading to a phase transition from the solid to the liquid and a color change from yellow to orange. The liquid *Z*-isomer can be pressed between two glass slides and irradiated with green light (λ = 520 nm) to revert the *Z*-AIZ to the *E*-AIZ, thereby solidifying and gluing the slides together.

designed, synthesized and studied. Their application as adhesives was evaluated and the observed results were attributed to their structural properties, helping to understand and overcome some of the challenges that this class of materials still faces in the field of adhesion. Ultimately, the results of this work shed light on the relationship between the demonstrated adhesive power and the chemical structure of the LMW, paving the way for further remarkable responsive adhesives (Fig. 1).

Results and discussion

In our previous work, AIZ were monosubstituted in the *para*-position to the azo bridge (Fig. 2). Aiming to understand the influence of the substitution pattern and to extend the knowledge about the influence of the substituent's chain length, we designed and synthesized a broad library of alkoxy-AIZ by initially permutating the position of two methoxy groups (Fig. 2, **1a–f**). Additionally, we synthesized longer chain dialkoxy- and trialkoxy-AIZ with pentoxy, hexoxy and nonoxy chains (Fig. 2, **2a–c**, and **3a–d**), as well as a short and long chain dialkoxy AAP (Fig. 2, **2d–e**), and compared their photophysical and adhesive properties with the monoalkoxy AIZ from the previous work. The AIZ have been synthesized according to Fig. S17–S19† and a detailed description of the synthesis and spectroscopic analysis can be found in the ESI.†

Most of the synthesized AIZ demonstrate the photoresponsive behavior in solution that is typical for azo compounds. The initial spectrum of 3,4-dimethoxy-AIZ (**1a**) shows a pronounced absorbance in the area of λ = 355 nm due to the π–π* transition and a much less pronounced absorbance in the area of λ = 440 nm due to the n–π* transition (Fig. 3a). Irradiation with UV-light (λ = 365 nm) brings the system to the metastable *Z*-isomer, resulting in a red-shift in absorption. Furthermore, the π–π* transition is weakened due to the reduced orbital overlap in the *Z*-isomer. Concomitantly, the n–π* transition around λ = 440 nm is enhanced in line with the very same geometrical changes. This phenomenon is reproducible over at least 10 cycles without any loss in the absorbance (Fig. 3a), underlining the photoreversibility of the system in solution alongside a thermal half-life of the *Z*-isomer of $\tau(20\ ^{\circ}C)_{1/2}$ = 207 d (Fig. S28†). These data also confirm the stability of AIZ to UV exposure.

However, for the application of the developed molecular photoswitches as adhesives, a solid state photoinduced solid-to-liquid phase transition is required. We therefore tested the photoisomerization for undissolved samples of **1a**. To our delight, compound **1a** was observed to undergo efficient photo liquefication upon irradiation with UV light starting as a solid powder (Fig. 4a) going through partial photo liquefication (Fig. 4b) until complete liquefication is achieved

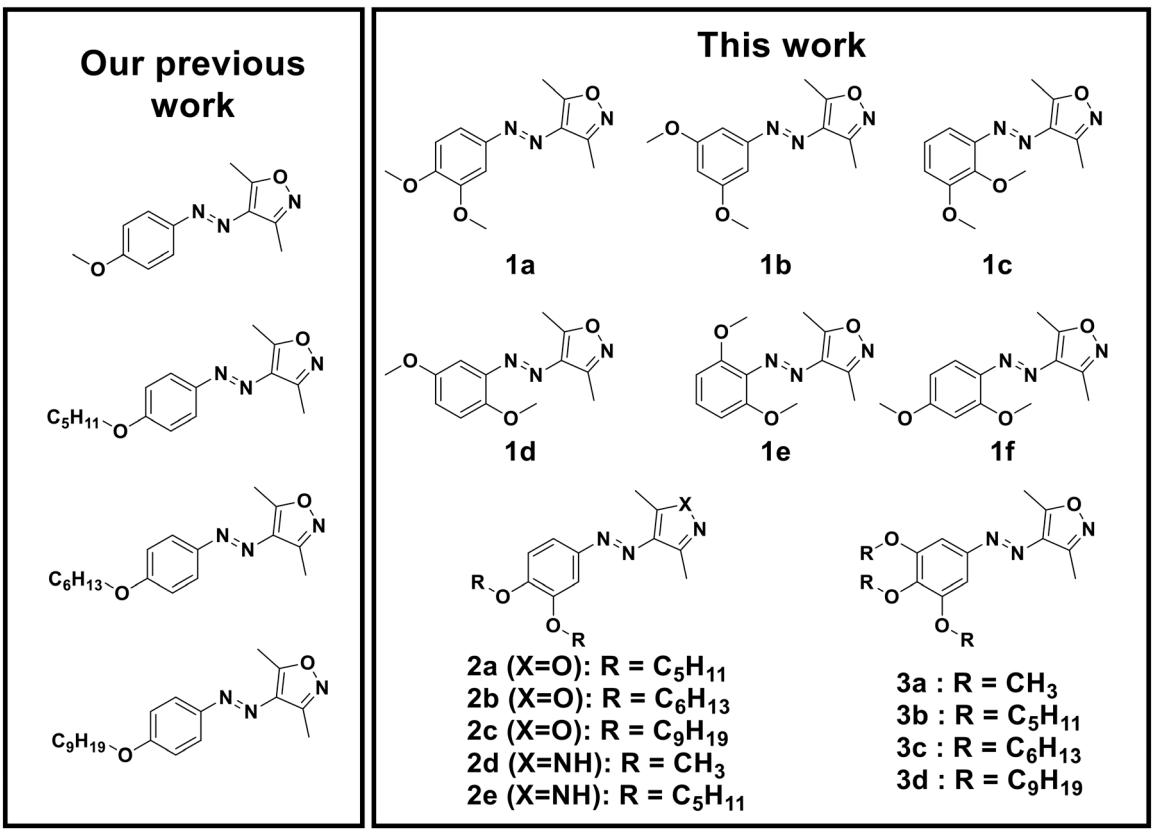

Fig. 2 Library of previously reported AIZ adhesives[11] and dimethoxy AIZ **1a–f**, dialkoxy AIZ **2a–c**, dialkoxy AAP **2d–e** and trialkoxy AIZ **3a–d** synthesized and analyzed in this work.

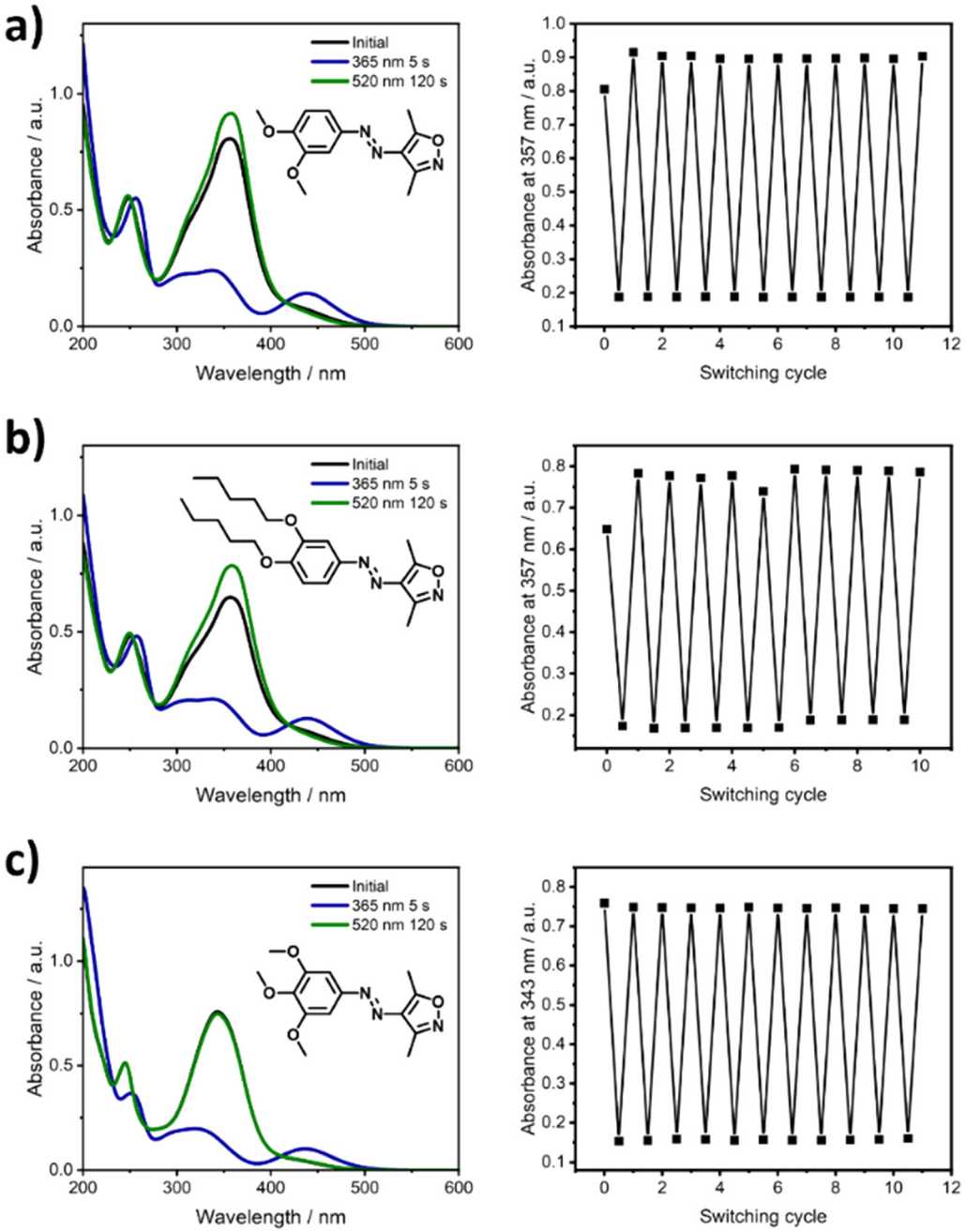

Fig. 3 UV/vis spectra of a) **1a**, b) **2a**, and c) **3a**, c = 50 μmol L^{-1} in acetonitrile, showing (left) the initial state (in black), after irradiation with UV light (λ = 365 nm) to form the *Z*-isomer (in blue) and after irradiation with green light (λ = 520 nm) to form the *E*-isomer (in green), as well as (right) the absorbance values at λ = 357 nm, or λ = 343 nm for trialkoxy-substituted AIZ **3a** for repeated switching (10 cycles).

(Fig. 4c). In turn, a phase reversion upon irradiation with green light was demonstrated resulting in a solid (Fig. 4d), showing potential for adhesive application. Adhesive tests were performed according to the protocol previously developed in our group[11] (for experimental details, see the ESI†). Use of **1a** as an adhesive resulted in a maximum weight-bearing capacity of 29.6 ± 2.0 N cm^{-2}. This is approximately five times higher than the 4-methoxy-substituted AIZ adhesive strength and comparable to the strongest AIZ adhesive from our previous work (4-pentoxy-substituted AIZ, 29.7 ± 0.1 N cm^{-2}),[11] showing a strong contribution of the second substituent on the adhesive properties. After photocuring and physically disjoining the adhering substrates, crystalline residues can be observed on the glass substrate *via* polarized light microscopy (as seen in Fig. S14 and S15†) underlining the effective liquid-to-solid phase transition triggered by light. The remarkable photoresponse of the adhesive can be seen in the video provided as ESI.† In the video, weights were attached slowly to two glass slides conjoined with **1a**, until a force of 14.1 N

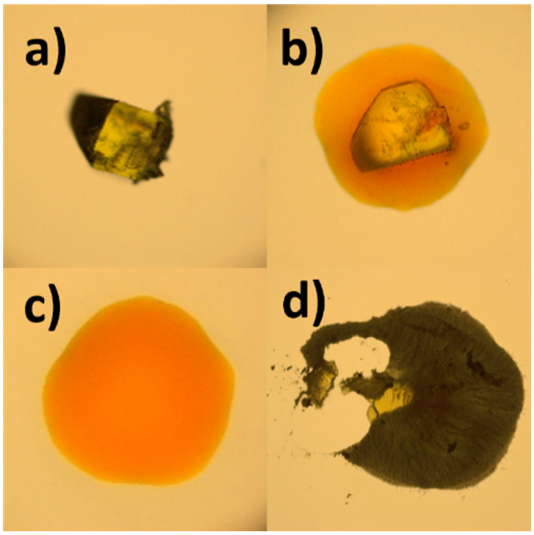

Fig. 4 Crystal of AIZ **1a** a) before and b) shortly after irradiation with UV-light (λ = 365 nm, 1 min) showing a partial UV-induced phase transition, c) fully liquefied after further irradiation with UV-light (λ = 365 nm, 1 min) and d) after recrystallization through irradiation with green light (λ = 520 nm, 5 min).

cm^{-2} is applied. After applying UV-light (λ = 365 nm), the slides are separated within 1.5 s.

Since crystallization behavior is often key to the adhesive properties, the crystal structure of **1a** was determined, revealing a triclinic structure (Fig. S20†). Furthermore, we compared the molecular packing of **1a** (3,4-dimethoxy-AIZ) with the previously published 4-methoxy-AIZ to understand the impressive difference in the adhesive strength. As seen in Fig. S26,† the 4-methoxy-AIZ does not show any π–π interactions between the phenyl rings, which are twisted relative to each other by around 48°. The most relevant interaction between the molecules in the crystal occurs between the pyrazole rings. In comparison, AIZ **1a** shows interactions between phenyl rings as well as pyrazole rings, resulting in a more ordered crystalline packing and enhanced π–π interactions (as seen in Fig. S27†). We assume that the more ordered crystalline structure results in an increased adhesive strength.

Notably, the melting point of **1a** is 102 °C, which is comparable to the melting point of the 4-methoxy-substituted AIZ (100 °C) and significantly higher than the pentoxy derivative (60 °C), extending the application window of this potent new adhesive.

Of note, in all gluing experiments the cohesion was stronger than the adhesion, resulting in a rupture at the interface, *i.e.*, between the adhesive layer and one of the glass substrates, rather than a failure in the structural integrity of the adhesive itself. Since the adhesion was found to be limiting, it may be possible to enhance the adhesive strength further by improving the interfacial contact. While a small loss of the adhesive cannot be avoided upon physical rupture, the majority of the used compound was found to remain on one of the glass slides and could be reused in the next gluing cycle. All adhesive systems were therefore tested in terms of their reversibility using the prepared substrates for 10 cycles, yielding a reversible adhesive strength with small fluctuations (below 20%) in the weight-bearing capacity and no negative trend could be seen, underlining the remarkable reusability of this class of adhesives.

To understand how different substitutions can influence the adhesive strength of the AIZ, a range of dimethoxy-AIZ (seen in Fig. 2 **1a–f**) were synthesized and analyzed in a similar manner as described above. 3,5-dimethoxy-AIZ (**1b**) shows photophysical properties similar to AIZ **1a** (Fig. S1†). A complete and rapid solid-to-liquid phase transition can be observed, but thermal re-isomerization occurs within seconds, limiting the compound's use as an adhesive. Nevertheless, such fast re-isomerization may have advantages in different applications, *e.g.*, self-healing surfaces. Besides showing behavior in solution comparable to **1a**, the other dimethoxy-AIZ (**1c–f**) exhibited a similar lack of adhesive behavior (Fig. S1†). A solid-to-liquid phase transition could be observed to some extent but the photostationary state did not yield a high enough conversion for an adhesive layer to successfully establish. AIZ **1e**, specifically, showed a photoresponsive behavior upon irradiation with UV light (λ = 365 nm), but reversion to the *E*-isomer was achieved through irradiation with blue light (λ = 434 nm) instead of the usual green light (λ = 520 nm) (Fig. S1†). All relevant UV/vis spectra can be found in Fig. S1.†

Since 3,4-dimethoxy-AIZ showed the most promising adhesive properties, we decided to further examine this substitution pattern and analyzed the corresponding pentoxy-, hexoxy- and nonoxy-AIZ, which were synthesized starting from the 3,4-dimethoxy-AIZ *via* deprotection of the hydroxy group and coupling of the alkyl chain in this position (see Fig. S19†). All synthesized 3,4-dialkoxy-AIZ demonstrated a promising switching behavior in UV/vis absorption spectra as well as a solid-to-liquid and liquid-to-solid phase transition upon irradiation with UV light (λ = 365 nm) and green light (λ = 520 nm) (Fig. 3b and S2†). The adhesive strength was determined using the same approach as before, showing once again an improvement upon the addition of a second alkoxy group to the phenyl ring (Fig. 5). In comparison with the corresponding mono-alkoxy AIZ (4-methoxy-AIZ 5.9 ± 0.7 N cm^{-2}; 4-hexoxy-AIZ 7.0 ± 0.5 N cm^{-2}), the adhesive strength could be increased by a factor of 4 or 5 (29.6 ± 2.0 N cm^{-2} for 3,4-dimethoxy-AIZ (**1a**) and 31.5 ± 3.3 N cm^{-2} for 3,4-dihexoxy-AIZ (**2b**)). Interestingly, the adhesive that showed the best performance in the previous study, 4-pentoxy-AIZ, exhibited a subtle 11% increase from 29.7 ± 0.1 N cm^{-2} to 33.0 ± 2.2 N cm^{-2} for 3,4-dipentoxy-AIZ (**2a**) to be on par with the other dialkoxy adhesives, suggesting that there is a limit in increasing the adhesive's strength through this modification. Contrary to the trend, 3,4-dinonoxy-AIZ (**2d**) has a lower adhesive strength than the 4-nonoxy-AIZ (25.2 ± 1.0 N cm^{-2} to 21.6 ± 2.2 N cm^{-2}), hinting that the gain from adding a second side-chain is limited to the lower chain lengths.

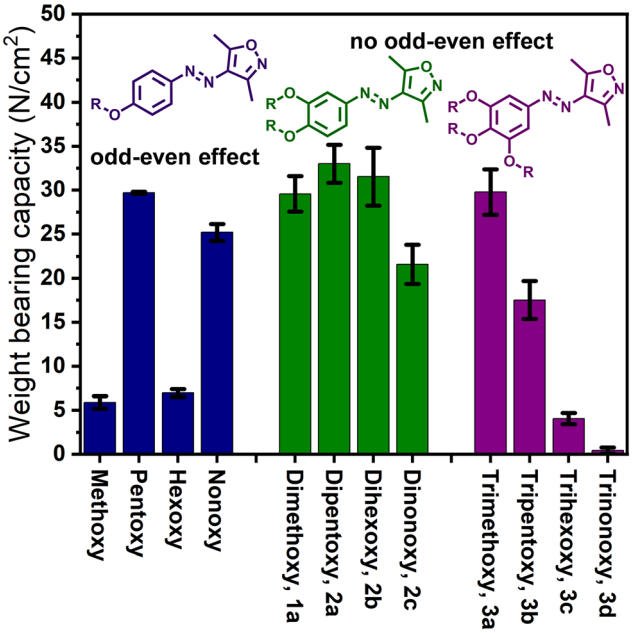

Fig. 5 Weight-bearing capacities of the synthesized alkoxy AIZ in comparison to the previously published ones.[11]

Next, we were interested if the addition of a third heterosubstituent to the phenyl ring would result in even more impressive adhesive properties. For this purpose, 3,4,5-trimethoxy-AIZ (**3a**) was synthesized starting from the trimethoxy-amine according to the procedure described in Fig. S17,† and the precursors for the longer-chain 3,4,5-trialkoxy-AIZ were synthesized through an alternative route due to the poor stability of the trihydroxy-AIZ (Fig. S18†).

The resulting 3,4,5-trialkoxy-AIZ demonstrated typical photoisomerization in solution (Fig. 3c and S3†). Longer chain 3,4,5-trihexoxy-AIZ (**3c**) and 3,4,5-trinonoxy-AIZ (**3d**) possessed melting points only slightly above room temperature (39 °C for 3c and 31 °C for **3d**, Fig. S33†), which is why visible light irradiation was not accompanied by immediate recrystallization, despite an apparent color change indicating reversible photoisomerization. 3,4,5-tripentoxy-AIZ (**3b**), on the other hand, could be used as an adhesive at room temperature, showing an adhesive strength of 17.5 ± 2.2 N cm^{-2}. With this number being lower than both the 4-pentoxy-AIZ as well as the 3,4-dipentoxy-AIZ, we concluded that the introduction of additional alkoxy-substituents to the AIZ core does not benefit the adhesive strength and may instead even weaken the crystallinity by further lowering its melting point. This could be observed as well in the adhesive strengths of 3,4-dihexoxy-AIZ (**3c**) and 3,4-dinonoxy-AIZ (**3d**) with 4.1 ± 0.6 N cm^{-2} (**3c**) and 0.4 ± 0.3 N cm^{-2} (**3d**), respectively, after cooling the conjoined glass slides to stimulate recrystallization after reisomerization to the *E*-AIZ. All in all, compound **3a**, the 3,4,5-trimethoxy-AIZ, once again showed the greatest improvement in its solid-to-liquid phase transitioning, yielding a maximum weight bearing capacity of 29.8 ± 2.6 N cm^{-2}, roughly identical to that of the 3,4-dimethoxy-AIZ.

In our previous report, a correlation between the odd–even effect and the adhesive strength was reported, yielding higher adhesive strengths with substituents having an even number of CH_2-groups (namely, 4-pentoxy-AIZ and 4-nonoxy-AIZ).[11] Attributed to the tighter packing of an even number of CH_2 spacers,[32] this effect seems to become less important after the addition of a second alkoxy substituent, as no significant difference in the adhesive strength is observed between the 3,4-dipentoxy-AIZ and 3,4-hexoxy-AIZ (Fig. 5). The effect of tighter packing between single alkyl chains with even-numbered CH_2 groups seems to decrease after the addition of the second and third alkyl chains on one AIZ, with the latter additionally showing a steep decrease in the adhesive strength with increasing chain lengths. Indeed, crystal structures could only be determined for the methoxy-substituted compounds **1a-b**, **1d–f** and **3a** (as seen in Fig. S20–S25†), but not for the longer-chain di- and trialkoxy-AIZ that did not demonstrate sufficient crystallization.

In an additional experiment, we compared two of the strongest adhesives of this study, 3,4-dimethoxy-AIZ (**1a**) and 3,4-dipentoxy-AIZ (**2a**), with their counterparts from another class of azo photoswitches, AAPs. Like the AIZ, AAPs generally exhibit efficient and near-to-complete photoisomerization and high photostationary states and are used in a variety of different stimuli-responsive systems, including liquid crystals[33] and polymeric adhesives.[8] 3,4-dimethoxy-AAP (**2d**) and 3,4-dipentoxy-AAP (**2e**) were prepared starting from the corresponding amines, and both exhibited the expected switching behavior in solution (Fig. S2†). However, the irradiation of the crystals of **2d** and **2e** with UV light (λ = 365 nm) resulted only in a partial phase transition, which is enough to change the morphology from needle-like crystals to round ones (as seen in Fig. S16†), but not yielding a full phase transition to the liquid phase. Apparently, the solid-state switching does not happen to a sufficient degree or the re-isomerization back to the *E*-isomer is taking place too rapidly, which hinders their use as an adhesive. Nevertheless, Kumar *et al.* could show that specific AAP derivatives can undergo a UV light-induced phase transition,[34] hinting that further variation of the molecular structure could enable the application of AAPs as reversible adhesives.

Experiments

Materials

All used chemicals were purchased from Merck KGaA (Darmstadt, Germany), BLD Pharmatech Ltd. (Shanghai, China), and TCI Europe (Zwijndrecht, Belgium) and were used without further purification.

Synthesis and characterization

The compounds were synthesized through modified literature procedures[2,11,35] as seen in Fig. S17–S19 in the ESI.† NMR spectra were recorded on Bruker AV300 (300 MHz) and Bruker AV400 (400 MHz) spectrometers (Bruker

Corporation, Billerica, USA) and the chemical shifts were referenced to internal standards. UV/vis absorption spectra were recorded with a V-770 double beam spectrophotometer (JASCO Gmbh, Pfungstadt, Germany). DSC measurements were conducted on a DSC 204 (NETZSCH-Gerätebau GmbH, Selb, Germany).

Conclusions and outlook

Inspired by our previous work on monoalkoxy-substituted AIZ LMW adhesives,[11] a broad library of di- and tri-substituted alkoxy AIZ was designed, synthesized, and thoroughly investigated for their adhesive properties. We identified a preference for dimethoxy substitution in the 3,4-position and achieved an increase in the adhesive strength of approximately 520% when compared to the 4-methoxy AIZ derivative. Interestingly, increasing the alkoxy chain length to 5 and 6 carbons yielded roughly identical adhesive strengths, exhibiting a slight improvement over the 4-pentoxy AIZ, which was previously shown to possess the highest adhesive strength among the monosubstituted AIZ. Increasing the chain length further resulted in a decrease in the adhesive strength that was also observed in the monosubstituted AIZ on account of the melting point being critically close to room temperature. In fact, this effect was also observed in the lower melting-point trialkoxy AIZ, with only trimethoxy AIZ reaching an adhesive strength comparable to the dialkoxy AIZ.

In summary, our findings reinforce that the AIZ family is highly suitable for application as photoreversible LMW adhesives. To the best of our knowledge, AIZ are the only azo heteroarenes that achieve good adhesive performance for a range of derivatives. Overall, the pronounced enhancement of the adhesive strength in the monomethoxy and monohexoxy AIZ adhesives upon extension to 3,4-disubstitution, in particular, underlines the importance of the tailored molecular design of LMW adhesives to achieve desired macroscopic properties. Furthermore, the adhesives can be recycled multiple times and (based on our previous report on monoalkoxy-substituted AIZ)[11] can likely be applied on various substrates other than glass.

Data availability

The data supporting this article have been included as part of the ESI.†

Conflicts of interest

The authors declare no competing interests.

Acknowledgements

We thank Dr. Henning Klaasen for helpful remarks and corrections.

References

1 (*a*) I. Strehin, Z. Nahas, K. Arora, T. Nguyen and J. Elisseeff, *Biomaterials*, 2010, **31**, 2788; (*b*) S. Hong, K. Yang, B. Kang, C. Lee, I. T. Song, E. Byun, K. in Park, S.-W. Cho and H. Lee, *Adv. Funct. Mater.*, 2013, **23**, 1774.
2 L. Stricker, E.-C. Fritz, M. Peterlechner, N. L. Doltsinis and B. J. Ravoo, *J. Am. Chem. Soc.*, 2016, **138**, 4547.
3 (*a*) I. Ali, L. Xudong, C. Xiaoqing, J. Zhiwei, M. Pervaiz, Y. Weimin, L. Haoyi and M. Sain, *Mater. Sci. Eng., C*, 2019, **103**, 109852; (*b*) M. Ali, T. Ueki, D. Tsurumi and T. Hirai, *Langmuir*, 2011, **27**, 7902; (*c*) J. Ping, F. Gao, J. L. Chen, R. D. Webster and T. W. J. Steele, *Nat. Commun.*, 2015, **6**, 8050; (*d*) M.-H. Zhang, C.-H. Li and J.-L. Zuo, *J. Chem. Eng.*, 2022, **433**, 133840.
4 A. Gibalova, L. Kortekaas, J. Simke and B. J. Ravoo, *Chem. – Eur. J.*, 2023, **29**, e202302215.
5 A. Gibalova, N. B. Arndt, L. Burg and B. J. Ravoo, *ACS Appl. Mater. Interfaces*, 2023, **15**, 12363.
6 N. R. Martinez Rodriguez, S. Das, Y. Kaufman, J. N. Israelachvili and J. H. Waite, *Biofouling*, 2015, **31**, 221.
7 (*a*) M. T. Northen, C. Greiner, E. Arzt and K. L. Turner, *Adv. Mater.*, 2008, **20**, 3905; (*b*) D. R. King, M. D. Bartlett, C. A. Gilman, D. J. Irschick and A. J. Crosby, *Adv. Mater.*, 2014, **26**, 4345.
8 S. Lamping, L. Stricker and B. J. Ravoo, *Polym. Chem.*, 2019, **10**, 683.
9 R. Göstl, A. Senf and S. Hecht, *Chem. Soc. Rev.*, 2014, **43**, 1982.
10 S. Crespi, N. A. Simeth and B. König, *Nat. Rev. Chem.*, 2019, **3**, 133.
11 L. Kortekaas, J. Simke, D. W. Kurka and B. J. Ravoo, *ACS Appl. Mater. Interfaces*, 2020, **12**, 32054.
12 C. E. Weston, R. D. Richardson, P. R. Haycock, A. J. P. White and M. J. Fuchter, *J. Am. Chem. Soc.*, 2014, **136**, 11878.
13 (*a*) M. Kathan and S. Hecht, *Chem. Soc. Rev.*, 2017, **46**, 5536; (*b*) L. Kortekaas and W. R. Browne, *Chem. Soc. Rev.*, 2019, **48**, 3406; (*c*) M. M. Lerch, W. Szymański and B. L. Feringa, *Chem. Soc. Rev.*, 2018, **47**, 1910.
14 G. S. Hartley, *Nature*, 1937, **140**, 281.
15 A. Mukherjee, M. D. Seyfried and B. J. Ravoo, *Angew. Chem., Int. Ed.*, 2023, **62**, e202304437.
16 N. Delorme, J.-F. Bardeau, A. Bulou and F. Poncin-Epaillard, *Langmuir*, 2005, **21**, 12278.
17 S. Ito, A. Yamashita, H. Akiyama, H. Kihara and M. Yoshida, *Macromol*, 2018, **51**, 3243.
18 P. Weis, A. Hess, G. Kircher, S. Huang, G. K. Auernhammer, K. Koynov, H.-J. Butt and S. Wu, *Chem. – Eur. J.*, 2019, **25**, 10946.
19 F. Höglsperger, B. E. Vos, A. D. Hofemeier, M. D. Seyfried, B. Stövesand, A. Alavizargar, L. Topp, A. Heuer, T. Betz and B. J. Ravoo, *Nat. Commun.*, 2023, **14**, 3760.
20 (*a*) Q. Qiu, Y. Shi and G. G. D. Han, *J. Mater. Chem. C*, 2021, **9**, 11444; (*b*) Y. Shi, M. A. Gerkman, Q. Qiu, S. Zhang and G. G. D. Han, *J. Mater. Chem. A*, 2021, **9**, 9798.

21 (*a*) J. Simke, T. Bösking and B. J. Ravoo, *Org. Lett.*, 2021, **23**, 7635; (*b*) D. Bléger and S. Hecht, *Angew. Chem., Int. Ed.*, 2015, **54**, 11338.
22 T. Wendler, C. Schütt, C. Näther and R. Herges, *J. Org. Chem.*, 2012, **77**, 3284.
23 (*a*) F. Stojcevski, O. Siddique, G. Meric, J. D. Randall, N. S. Emonson and L. C. Henderson, *Int. J. Adhes. Adhes.*, 2021, **104**, 102740; (*b*) R. Bourgi, L. Hardan, A. Rivera-Gonzaga and C. E. Cuevas-Suárez, *Int. J. Adhes. Adhes.*, 2021, **105**, 102794.
24 X. Luo, K. E. Lauber and P. T. Mather, *Polymer*, 2010, **51**, 1169.
25 P. Weis, W. Tian and S. Wu, *Chem. – Eur. J.*, 2018, **24**, 6494.
26 S. Ito, H. Akiyama, R. Sekizawa, M. Mori, T. Fukata, M. Yoshida and H. Kihara, *J. Polym. Sci., Part A: Polym. Chem.*, 2019, **57**, 806.
27 Y. Zhou, C. Zhang, S. Gao, B. Zhang, J. Sun, J. Kai, B. Wang and Z. Wang, *Chem. Mater.*, 2021, **33**, 8822.
28 (*a*) S. Dong, J. Leng, Y. Feng, M. Liu, C. J. Stackhouse, A. Schönhals, L. Chiappisi, L. Gao, W. Chen and J. Shang, *et al.*, *Sci. Adv.*, 2017, **3**, eaao0900; (*b*) X. Li, Y. Deng, J. Lai, G. Zhao and S. Dong, *J. Am. Chem. Soc.*, 2020, **142**, 5371.
29 (*a*) Y. Liang, K. Wang, J. Li, Y. Zhang, J. Liu, K. Zhang, Y. Cui, M. Wang and C.-S. Liu, *Mater. Horiz.*, 2022, **9**, 1700; (*b*) Y. Liang, K. Wang, J. Li, H. Wang, X.-Q. Xie, Y. Cui, Y. Zhang, M. Wang and C.-S. Liu, *Adv. Funct. Mater.*, 2021, **31**, 2104963.
30 (*a*) H. Akiyama and M. Yoshida, *Adv. Mater.*, 2012, **24**, 2353; (*b*) H. Akiyama, S. Kanazawa, Y. Okuyama, M. Yoshida, H. Kihara, H. Nagai, Y. Norikane and R. Azumi, *ACS Appl. Mater. Interfaces*, 2014, **6**, 7933; (*c*) S. Ito, H. Akiyama, R. Sekizawa, M. Mori, M. Yoshida and H. Kihara, *ACS Appl. Mater. Interfaces*, 2018, **10**, 32649.
31 P. Kumar, A. Srivastava, C. Sah, S. Devi and S. Venkataramani, *Chem. – Eur. J.*, 2019, **25**, 11924.
32 L. Kortekaas, J. Simke, N. B. Arndt, M. Böckmann, N. L. Doltsinis and B. J. Ravoo, *Chem. Sci.*, 2021, **12**, 11338.
33 H. Q. Trân, S. Kawano, R. E. Thielemann, K. Tanaka and B. J. Ravoo, *Chem. – Eur. J.*, 2024, **30**, e202302958.
34 H. Kumar, G. Parthiban, A. Velloth, J. Saini, R. De, S. K. Pal, K. S. Hazra and S. Venkataramani, *Chem. – Eur. J.*, 2024, e202401836.
35 (*a*) M. R. Molla, A. Das and S. Ghosh, *Chem. – Eur. J.*, 2010, **16**, 10084; (*b*) A. Das and S. Ghosh, *Chem. – Eur. J.*, 2010, **16**, 13622; (*c*) A. Das and S. Ghosh, *Chem. Commun.*, 2011, **47**, 8922.